J Geophys (1982) 50:194–201

Journal of Geophysics

Joint Two-Dimensional Observations of Ground Magnetic and Ionospheric Electric Fields Associated with Auroral Currents

5. Current System Associated with Eastward Drifting Omega Bands

Dieter André [1]* and Wolfgang Baumjohann [2]

[1] Max-Planck-Institut für Aeronomie, Postfach 20, D-3411 Katlenburg-Lindau 3, Federal Republic of Germany
[2] Institut für Geophysik der Universität Münster, Corrensstr. 24, D-4400 Münster, Federal Republic of Germany

Abstract. Magnetograms from the Scandinavian Magnetometer Array (SMA) and ionospheric electric field measurements from the Scandinavian Twin Auroral Radar Experiment (STARE) have been evaluated during the passage of several omega bands (or eastward travelling surges) over Northern Scandinavia around 0400 MLT on 16 February 1977. The eastward motion of the omega bands was a pure $E \times B$ drift and was associated with Ps6 disturbances of the east-west component particularly of magnetic and electric fields. The two-dimensional distributions of electric and magnetic disturbance fields strongly support the hypothesis of a three-dimensional current system which is embedded in a rather homogeneous westward Hall current and where north-south aligned localized regions of field-aligned currents, flowing upward close to the omega band's wave-crest and downward east and west of it, are travelling eastward with the omega band. These field-aligned currents are associated with eastward and westward electric field disturbances and southward and northward Hall currents between them. It remains unclear whether these Hall currents close within the ionosphere, i.e. forming counterclockwise and clockwise ellipsoidal Hall current vortices, or if they diverge from the ionosphere as field-aligned currents at the southern and northern boundary of the region that is disturbed by the omega band.

Key words: Scandinavian Magnetometer Array – STARE – Magnetic fields – Electric fields – Auroral zone – Omega bands – Eastward travelling surges – Ps6

Introduction

In his review paper on auroral forms Akasofu (1974) defines omega bands as a wavy structure of the poleward auroral boundary with the shape of a series of Ω open to the pole, appearing most often in the local morning or midnight sector and generally drifting eastward (therefore the term "eastward travelling surge" is also used). We have started from this definition to determine a period when omega bands occurred and have then evaluated the STARE and magnetometer data for this time. This means that our classification is different from that of earlier papers, which describe mainly a certain class of magnetic variations, and may thereby also include events that are not connected to omega bands.

A comparison of our magnetic variations show a certain similarity to the Ps6 described by Saito (1974, 1978) and with eastward travelling disturbance described by Kawasaki and Rostoker (1979) and Gustafsson et al. (1981). Saito infers that Ps6 are caused by substorms and generated by a wavelike motion of the electrojet travelling eastward in the morning sector. Kawasaki and Rostoker (1979) have modelled their disturbances by a system of travelling field-aligned currents closing in the north-south direction. Gustafsson et al. (1981) reproduced their equivalent current pattern by Hall current vortices around an east-west aligned pair of line-type field-aligned currents.

Since, in contrast to these earlier measurements, we have two-dimensional measurements of ground magnetic and ionospheric electric fields, we are – as in earlier papers of this series (Baumjohann et al. 1980; 1981; Baumjohann and Kamide 1981; Inhester et al. 1981) – able not only to verify that our measurements belong to the same class of events, but can decide which model is the real one.

Instrumentation

The sites of the SMA-magnetometers (Scandinavian Magnetometer Array) used for this study are shown in Fig. 1. Most of the instruments are located along six roughly parallel, north-south profiles. A detailed description of this magnetometer network has been given by Küppers et al. (1979) and, for profile 5, by Maurer and Theile (1978). The coordinate system indicated in Fig. 1 has been introduced by Küppers et al. (1979) and has been named the Kiruna system. It is a Cartesian system obtained by a stereographic projection of the globe onto a tangential plane centered at Kiruna, Sweden (67.8° N, 20.4° E). The y_{KI} axis of the system has been chosen as the tangent to the projection of the line ϕ_c (KIR) = 64.8° with ϕ_c denoting the revised corrected geomagnetic latitudes as given by Gustafsson (1970). The x_{KI} axis points approximately 12° west of geographic north at KIR.

Again referrring to Fig. 1, the area enclosed by the dashed trapezoid is the common region seen by the two STARE radars (Greenwald et al. 1978). The STARE radars are sensitive to electrostatic plasma waves in the auroral E region. These waves, often called irregularities, are produced by the combined effects of the two stream and gradient drift plasma instabilities (see Greenwald, 1974). Greenwald (1979) has summarized evidence that in the auroral E layer the net drift velocity of the irregularities is nearly a pure $E \times B$ drift. Hence, the transverse ionospheric electric field vector is orthogonal and proportional to the measured drift velocity vector. Strong experimental evidence for this relationship has been found by Ecklund et al. (1977), Cahill et al. (1978) and Zanetti et al. (1980).

* *Present address:* Siemens AG, Hofmannstr. 51, D-8000 München 70, Federal Republic of Germany

0340-062X/82/0050/0194/$01.60

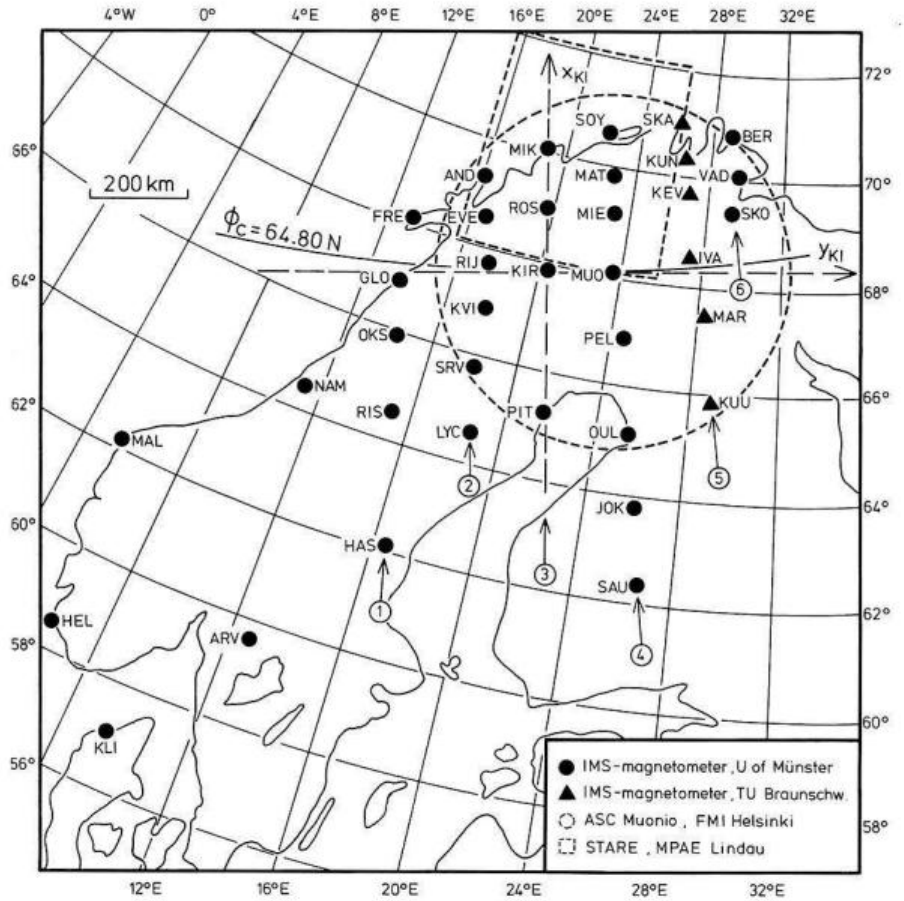

Fig. 1. Locations of the magnetic stations used in this study. The dashed trapezoid represents the common observation area of both STARE radars. The observational coverage of the Muonio all-sky camera is indicated by the *broken circle* (limited by an elevation angle of 15° and a height of 100 km). The axes define the Kiruna system (see text). The ringed *numbers* are the profile numbers of the six latitudinal magnetometer chains

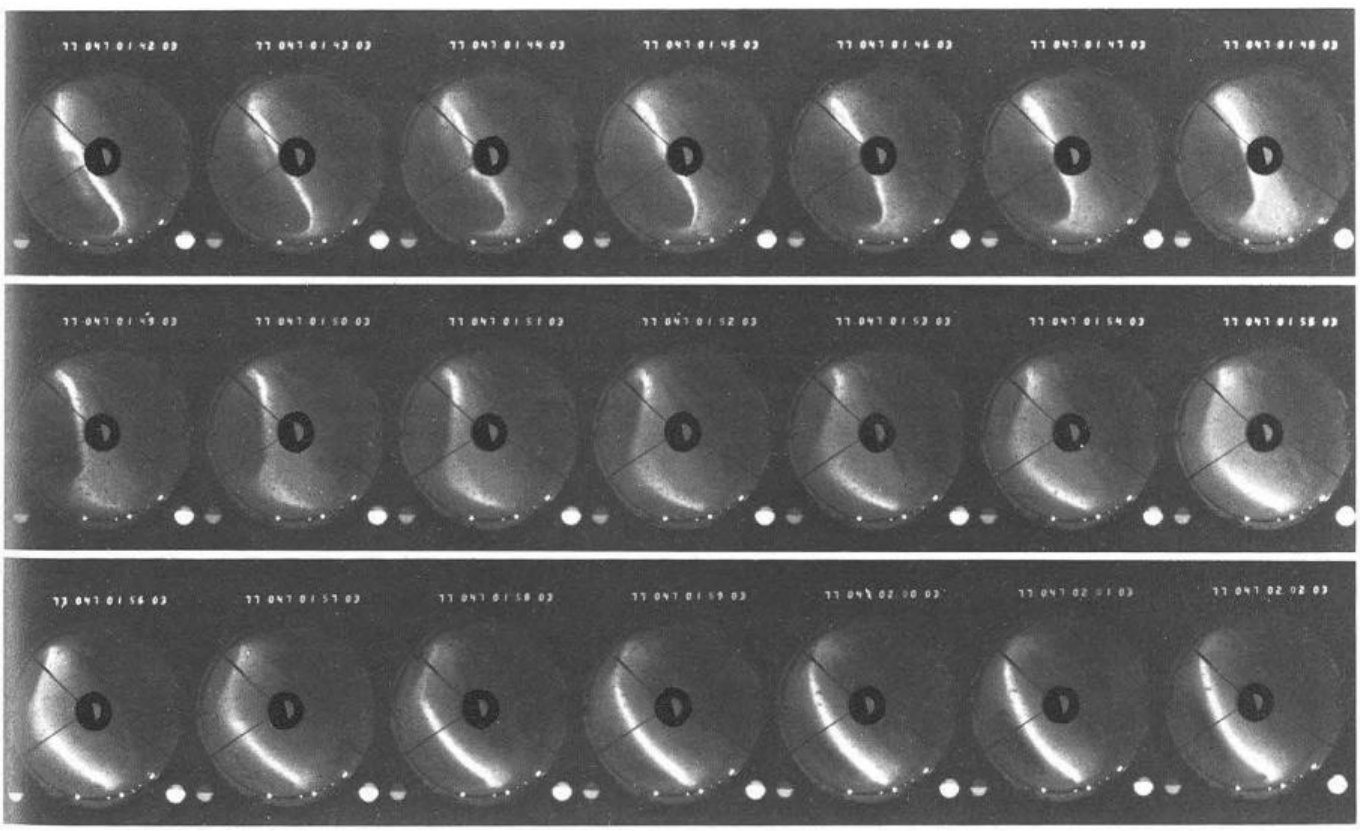

Fig. 2. Photographs taken by the all-sky camera at Muonio every minute between 0142 UT (*upper left corner*) and 0202 UT (*lower right corner*). Geographic north is to the left and geographic east to the top of the figure

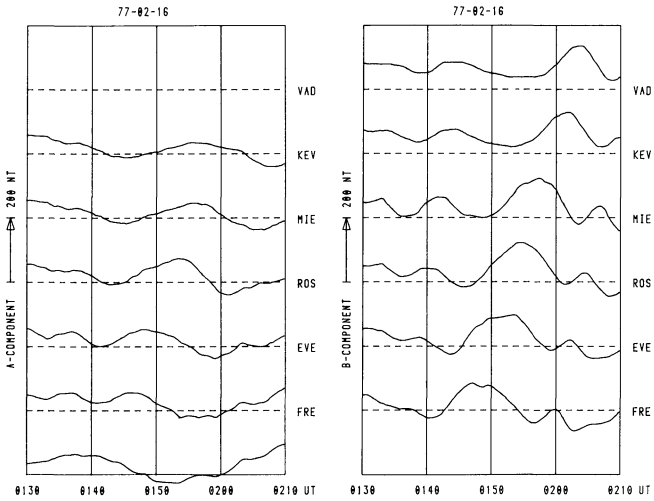

Fig. 3. Magnetograms of A and B components on a longitudinal profile (VAD-FRE, x_{KI}: +100 km, y_{KI}: +400 to −300 km). The A and B components are aligned along the x_{KI} and y_{KI} axes, respectively (see Fig. 1)

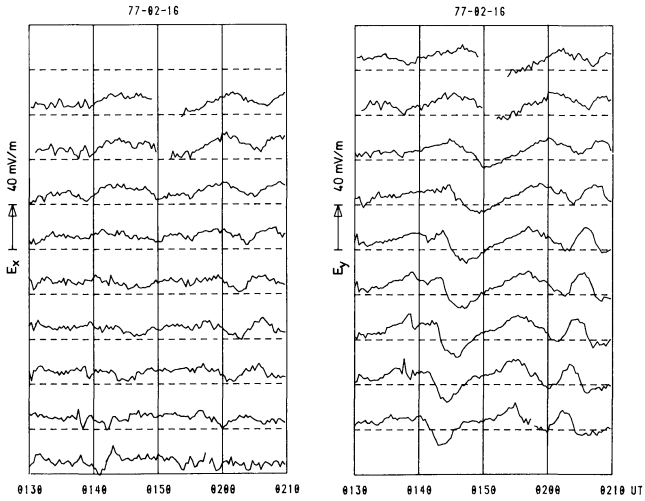

Fig. 4. Horizontal ionospheric electric field components (E_x and E_y are parallel to x_{KI} and y_{KI}, respectively) along a longitudinal profile at x_{KI} = +250 km. The corresponding y_{KI} coordinates are (from top): +250, +200, +150, +100, +50, 0, −50, −100, −150 km. The components displayed are averages of the STARE observations within a radius of 25 km around the grid point (exponentially weighted by their distance from the center). Gaps in the traces occur where the electric field magnitude was below the threshold level of 15–25 mVm^{-1}

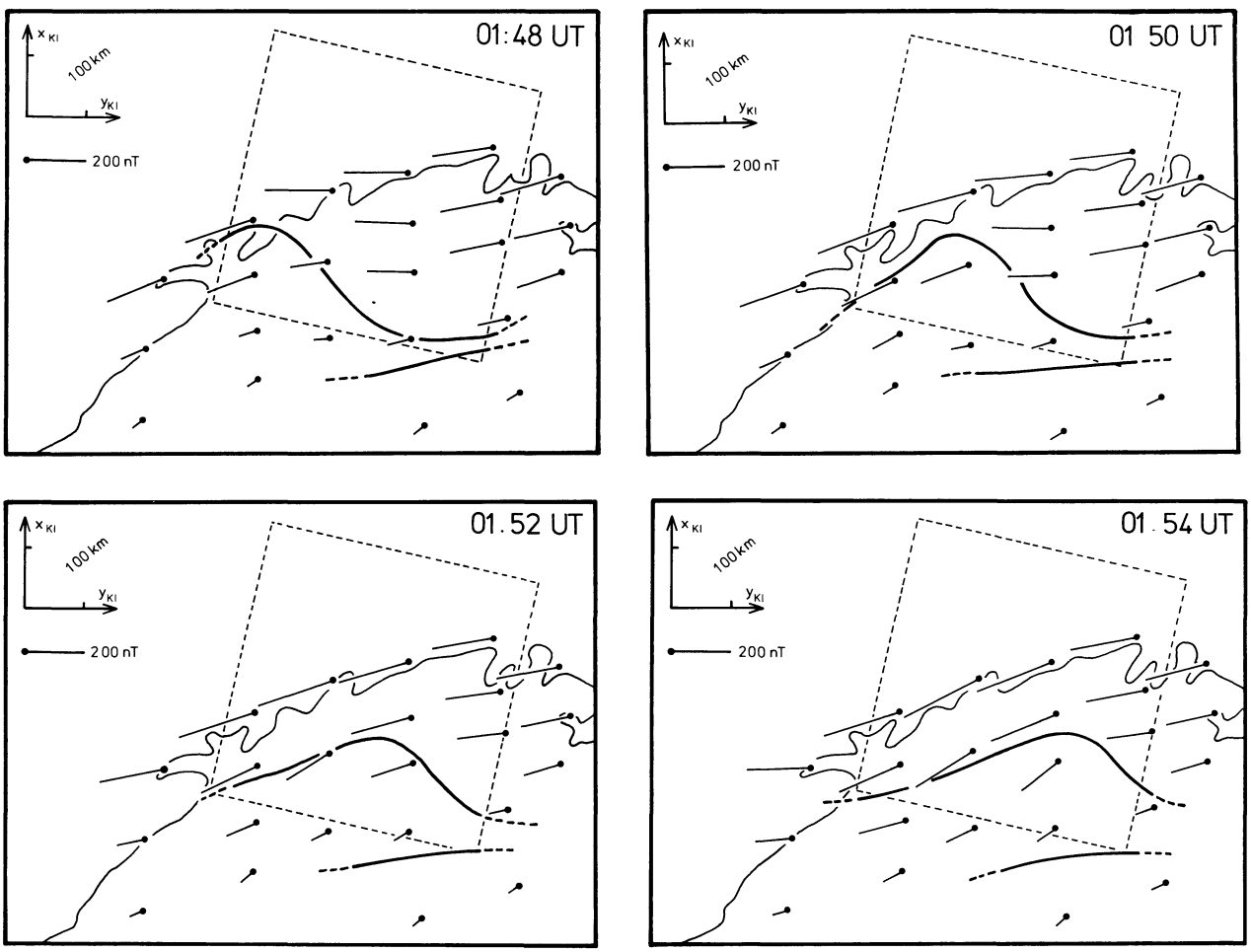

Fig. 5. Spatial distribution of equivalent current vectors on the ground and the lower boundary of the omega band (dashed where extrapolated) every 2 min between 0148 and 0154 UT The equivalent current vectors originate where the corresponding magnetic disturbance vectors were observed. The *dashed square* gives the location of the STARE frame for easier comparison with Fig. 6

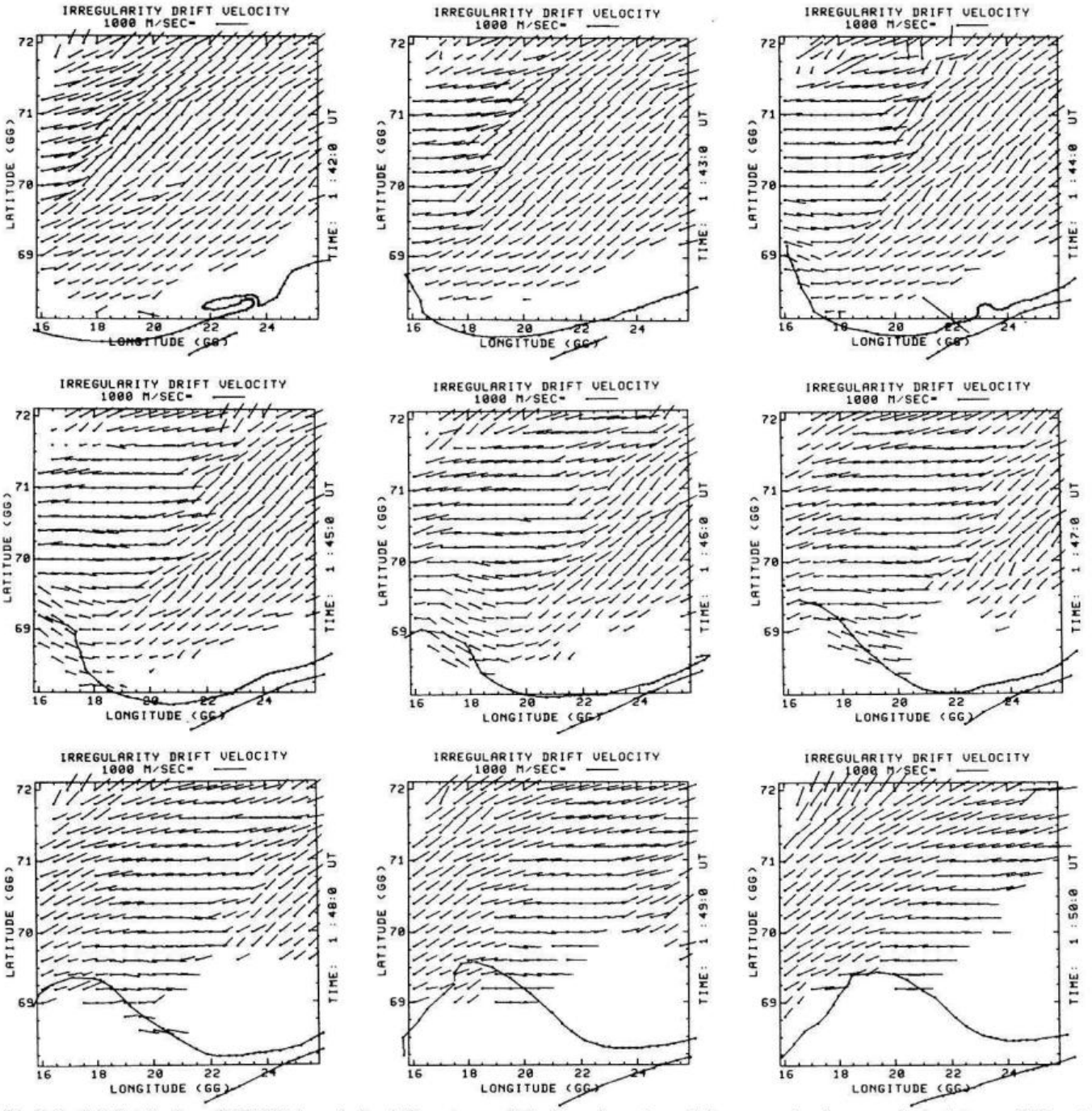

Fig. 6. Spatial distribution of STARE irregularity drift vectors and the lower boundary of the omega band every minute between 0142 and 0150 UT

The lower aurora boundary in the all-sky pictures of the camera at Muonio (Hyppönen et al. 1974) has been digitized, rectified and mapped into geographical coordinates and into the Kiruna system under the assumption that the lower boundary of the aurora is located at a height of 100 km (Boyd et al. 1971). The resulting error in the location if the true height is 10 km higher or lower than assumed may be estimated to about 20 km for a zenith distance of 70° (Opgenoorth et al. 1980).

Data Presentation and Analysis

Omega bands were drifting through the all-sky camera field of view from 0130 UT to 0230 UT on 16 February 1977 with an approximate speed of 40 km/min and a repetition period of 15 to 20 min. In Fig. 2 all-sky camera pictures taken during the passage of the most pronounced omega band are shown.

The whole structure looks like a wave moving eastward (after transformation into geographical or Kiruna coordinates this is even more pronounced). Omega bands occurring before and after this time have the same general appearance, but are less pronounced, in the magnetic and electric field variations.

The temporal development of the horizontal components of ground magnetic and ionospheric electric fields observed along the (longitudinal) y_{KI} axis are displayed in Figs. 3 and 4, respectively (A and E_x are parallel to x_{KI}, B and E_y are parallel to y_{KI}). Both magnetic and electric variations are clearly within

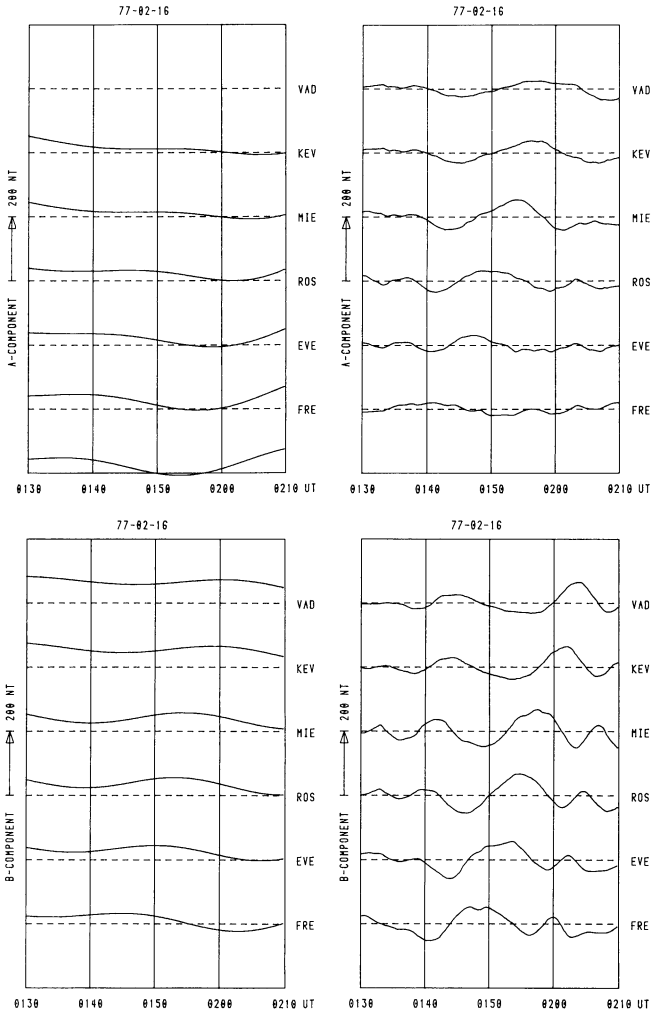

Fig. 7. Filtered magnetograms of A and B components displayed in Fig. 3. The low frequency traces (periods greater than 30 min) are given in the left-hand column while the higher frequency traces (periods less than 30 min) are given in the right-hand column

the Ps6 range (15–20 min) and were probably initiated by substorm activity west of Scandinavia before 0100 UT (see Baumjohann and Kamide 1981). As is usual for Ps6, the magnetic fluctuations are more pronounced in the (east-west) B component (Saito 1972; 1974; 1978; Kawasaki and Rostoker 1979; Gustafsson et al. 1981). The electric field also varies considerably more in the (east-west) E_y component, in agreement with the measurements of Gustafsson et al. (1981). It can also be seen clearly that the extrema are observed earlier at the western stations and that they are travelling eastwards with the same velocity as the omega bands, i.e. about 40 km/min.

The relation between the omega bands and the disturbances in magnetic and electric fields can be seen even more clearly in Figs. 5 and 6, where we show the two-dimensional distribution of equivalent current vectors and STARE drift velocities together with the auroral boundary during the passage of the most pronounced omega band over Scandinavia. The STARE data show a rather sharply bounded region of eastward drift embedded in the otherwise northeast drift. The region is about 150 km wide in longitude and extends 250 km to the northeast. It is moving with the omega band. The equivalent current vectors display a southwest orientation in the region of northeast irregularity drifts and westward equivalent current near the omega band wave-crest where STARE observed eastward drifts. This behaviour of irregularity drifts and current vectors is equivalent to the wavy motion of the polar electrojet that has been proposed by Saito (1978) as an explanation for Ps6 magnetic variations.

In order to analyze more accurately the disturbances of the background electric field and electrojet caused by the omega band, we have followed Gustafsson et al. (1981) and separated the Ps6 fluctuations from the more slowly varying contributions by filtering (with the -6dB cutoff point at a period of 30 min) magnetograms and electrograms measured by the SMA and STARE (some of these are shown in Figs. 3 and 4). The results of this filtering, i.e. the high frequency signal associated with the omega band and the low frequency signal associated with background electric field and electrojet, are shown in Figs. 7 and 8 for those traces displayed in Figs. 3 and 4. Since the STARE electrograms showed some very high frequency scatter as well as some data gaps due to subthreshold electric fields (Cahill et al. 1978) smooth cubic spline functions were fitted to the electrograms before filtering (these are also displayed in Fig. 8).

We will now concentrate on the most pronounced omega band that crossed northern Scandinavia between 0140 and 0200 UT (Figs. 3 and 4). This omega band travelled to the east with a velocity component $v_y = 670\ \mathrm{ms}^{-1}$ along the y_{KI} axis and had also a small northward velocity component $v_x = 85\ \mathrm{ms}^{-1}$ parallel to the x_{KI} axis. Figures 2, 3 and 4 show that the omega band maintains its shape during the traversal of northern Scandinavia. In addition, the irregularity drift and equivalent current vector fields obviously remain constant relative to the wave crest. This strongly suggests a stationary pattern for the omega band and the magnetic and electric perturbations related to it which drifts with the omega band. In order to display this behaviour clearly the (two-dimensional) total, the low frequency background, and the higher frequency disturbance vector field distributions measured between 0135 and 0205 UT were each superimposed with the moving omega band as a natural reference frame and averaged in $50 \times 50\ \mathrm{km}^2$ cells. The resultant vector distributions are shown in Fig. 9.

The magnetic and electric vector fields display quite clearly that the filtering in the time domain has actually resulted in a spatial filtering where whe have separated the total measured vector fields into a both temporally and spatially rather homogeneous background field which is very probably due to magnetospheric convection and a temporally and spatially inhomogeneous disturbance field that is associated with the omega band.

Additional Results and Discussion

In previous studies of eastward travelling disturbances mainly ground-based magnetic data were analysed and thus the different authors were not able to definitely discriminate between the two (following) different current systems that are both able to reproduce the higher frequency part of the magnetic variations on the ground:

1) Circular Hall current loops around line-type field-aligned currents in the centers of the vortices with no conductivity gradients in the ionosphere (Baumjohann 1979; Gustafsson et al. 1981).
2) A southward Cowling current flowing in a region of higher conductivity closed by field-aligned currents in the north and south (Baumjohann et al. 1977; Kawasaki and Rostoker 1979; Rostoker and Barichello 1980).

Our two-dimensional observations of ground-based magnetic and ionospheric electric fields allow us to infer the real nature

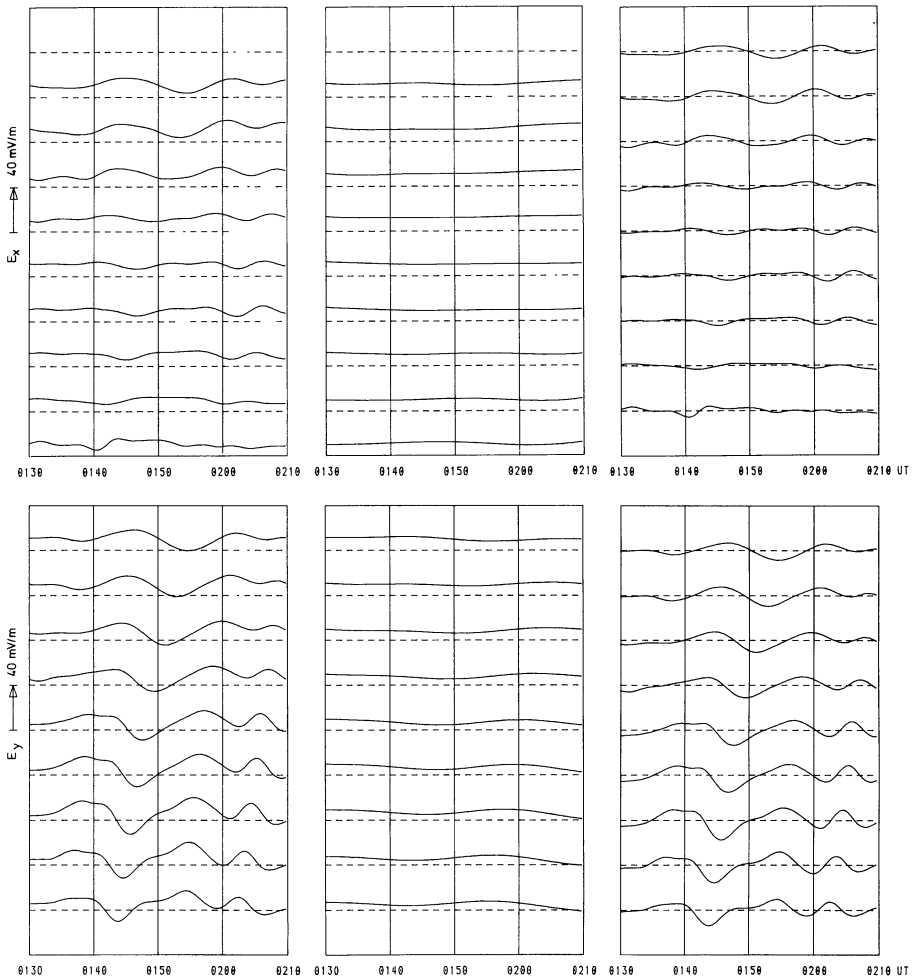

Fig. 8. Filtered electrograms of E_x (upper row) and E_y (lower row) components. The traces in the left-hand column have been obtained by fitting smooth cubic spline functions to the original data displayed in Fig. 4 in order to reduce very high frequency scatter and to fill data gaps due to subthreshold fields before filtering. Low frequency and higher frequency traces (periods greater/less than 30 min) are given in the middle and right-hand columns, respectively

of both the slowly varying and homogeneous background electrojet and the rather inhomogeneous currents associated with the omega band.

The low frequency background electric field has amplitudes of about -30 and $5\ \mathrm{mVm}^{-1}$ for the E_x and E_y components, respectively. These values are approximately the same as those found by Baumjohann and Kamide (1981) 1 h later on the same day after the omega bands have passed over Scandinavia and are also in good agreement with other electric field observations in this local time sector (Mozer and Lucht 1974; Madsen et al. 1976; Holzworth et al. 1977). The slowly varying background horizontal magnetic field and equivalent current were nearly exactly parallel and orthogonal, respectively, to the direction of the convection electric field, i.e. 12° eastward and northward from the negative x_{KI} and y_{KI} axes, respectively. This leads to the conclusion that the background westward electrojet is a Hall current flowing along the auroral oval that is typically also inclined by about 10°–15° against lines of constant magnetic latitude, i.e. the x_{KI} axis (Davis 1962; Gustafsson 1967; 1969; Meng et al. 1977; Lassen and Danielsen 1978; see Baumjohann and Kamide (1981) for a more thoroughly discussion of this topic).

The drift velocity vector of the omega band points about 10° eastward from the negative y_{KI} axis, i.e. perpendicular to the background electric field. Moreover, by comparing the drift velocity of the omega band $(v_x, v_y)=(85\ \mathrm{ms}^{-1}, 670\ \mathrm{ms}^{-1})$ with the horizontal background electric field components given above, it becomes obvious that the eastward motion of the omega band along the auroral oval is a pure $E\times B$ drift. The slightly too high velocity of the omega band as compared to the convection electric field measured by STARE in the earth-fixed frame may easily be attributed to the dynamo action of neutral winds in the ionosphere (Brekke et al. 1973; Comfort et al. 1976; Rino et al. 1977).

The electric field distribution associated with the omega band can be explained by a north-south aligned region of upward field-aligned currents and thus negatively charged field lines just north of the wave crest and of downward field-aligned currents and thus positively charged field lines east and west of the omega band (the electric charge dissipating as Pedersen currents in the ionosphere from the foot of the field lines is assumably compensated by field-aligned current from the magnetosphere; see Fukushima 1974). The location of the upward field-aligned current region corroborates the results of other studies on Ps6 and omega bands, which describe observations of strong riometer absorption and thus energetic electron precipitation that is supposed to carry upward field-aligned current (Kamide and Rostoker 1977; Theile and Wilhelm 1980) west of the southward equivalent current region (Gustafsson et al. 1981) and just east of the region of purely eastward total irregularity drift vectors (Oksman et al., personal communication 1981).

A comparison of the higher frequency electric and equivalent current vector fields shows that eastward and westward electric field vectors and southward and northward equivalent current vectors are nearly perpendicular to each other. This favours the Hall current vortex model against the southward Cowling current model. However, it remains unclear whether the Hall

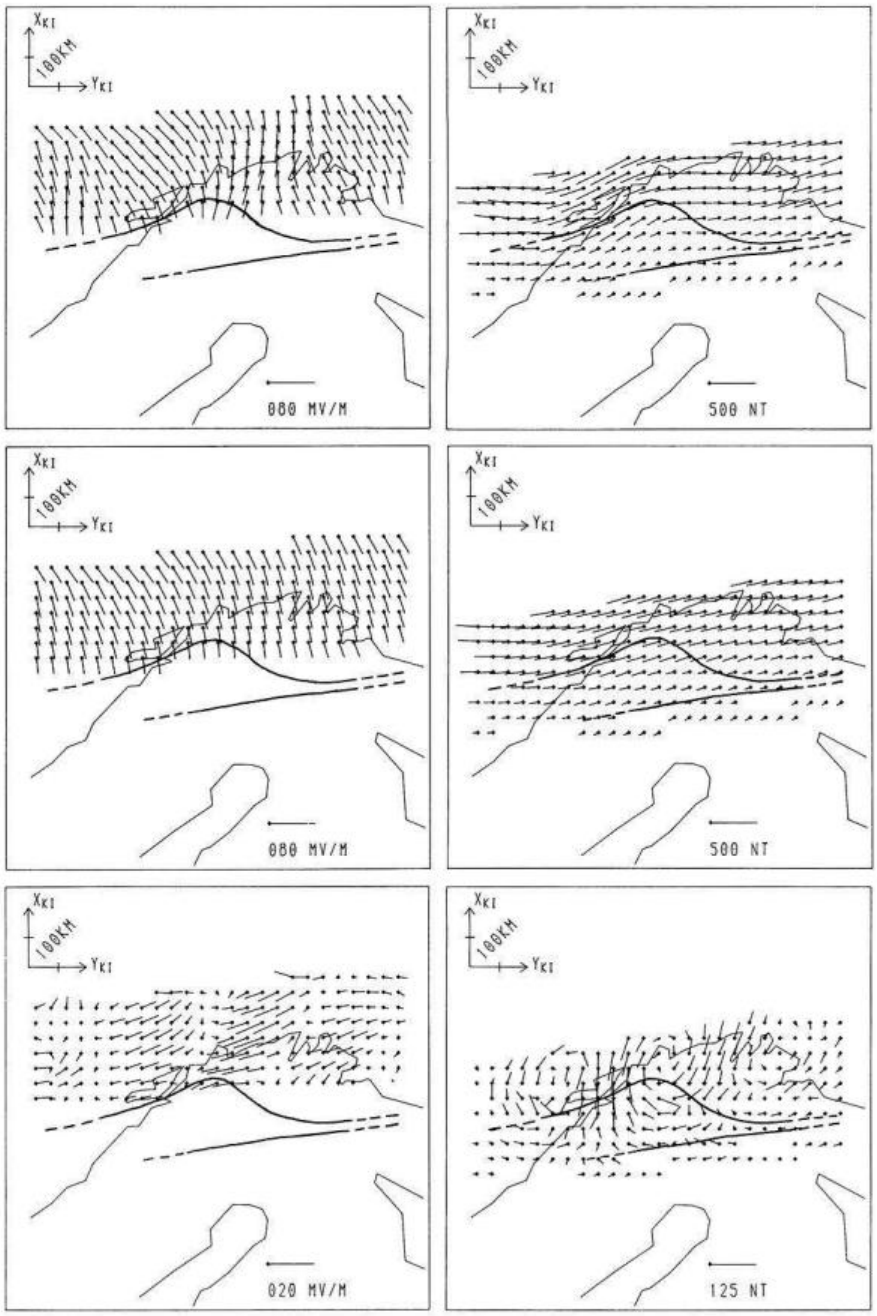

Fig. 9. Spatial distribution of electric field vectors (left-hand column) and equivalent current vectors on the ground (right-hand column) measured between 0135 and 0205 UT, superimposed and averaged in 50×50 km^2 cells under the assumption of a stationary pattern drifting with the omega band, whose average lower boundary has also been drawn in. The upper panel gives the unfiltered vector fields while middle and lower panels give lower and higher frequency components respectively. The outline of the Scandinavian coast is given relative to its location at 0150 UT

currents close within the ionosphere via east-west Hall currents or diverge from the ionosphere as field-aligned currents at the southern and northern boundary of the region that is disturbed by the omega band, since the electric field below the omega band's wave-creast was obviously too low to be detected by STARE and thus we are not able to decide if the eastward and westward equivalent currents in this region are Hall currents or if they are caused by the magnetic effect of field-aligned currents.

From the equivalent current vector distribution one can see that the Hall conductivity near and just behind the wave crest is somewhat enhanced, since the southward current vectors are comparatively bigger than the northward current vectors to the east. (note that this east-west aligned conductivity gradient is parallel to the electric field and to the gradient of the electric potential and thus, as in the case of homogeneous conductivity, only Hall currents are observed on the ground). The Hall conductivity enhancement is apparently caused by the precipitation of energetic electrons that carry the upward field-aligned current.

Acknowledgements. The magnetic observations were performed in cooperation with the Aarhus University, the Royal Institute of Technology at Stockholm, the Finnish Meteorological Institute at Helsinki, the University of Bergen, the Geophysical Observatory at Sodankylä, the Kiruna Geophysical Institute, the University of Oulu and the University at Tromsö. The STARE radars are operated with ELAB and the Norwegian Technical University in Trondheim and the Finnish Meteorological Institute in Helsinki. We thank these institutions and all members of the magnetometer group at the University of Münster and the STARE group at the MPAE for their support. We would also like to thank H. Maurer and T.U. Braunschweig for supplying us with magnetic data of the Braunschweig chain and R.J. Pellinen, FMI Helsinki, for making available the all-sky camera data. The magnetometer array observations and the work of W. Baumjohann were supported by grants from the Deutsche Forschungsgemeinschaft.

References

Akasofu, S.-I.: A study of auroral displays photographed from DMSP-2 satellite and from the Alaska meridian chain of stations. Space Sci. Rev. **16**, 617–725, 1974

Baumjohann, W.: Spatially inhomogeneous current configurations as seen by the Scandinavian Magnetometer Array. In: Proceedings of the International Workshop on Selected Topics of Magnetospheric Physics, Japanese IMS Committee, eds.: pp. 35–40. Tokyo 1979

Baumjohann, W., Kamide, K: Joint two-dimensional observations of ground magnetic and ionospheric electric fields associated with auroral zone currents. 2. Three-dimensional current flow in the morning sector during substorm recovery. J. Geomagn. Geoelectr. **33**, 297–318, 1981

Baumjohann, W., Gustafsson, G., Küppers, F.: Large-amplitude rapid magnetic variations during a substorm (abstract only). EOS Trans. AGU **58**, 718, 1977

Baumjohann, W., Untiedt, J., Greenwald, R.A.: Joint two-dimensional observations of ground magnetic and ionospheric electric fields associated with auroral zone currents. 1. Three-dimensional current flows associated with a substorm-intensified eastward electrojet. J. Geophys. Res. **85**, 1963–1978, 1980

Baumjohann, W., Pellinen, R.J., Opgenoorth, H.J., Nielsen, E.: Joint two-dimensional observations of ground magnetic and ionospheric electric fields associated with auroral zone currents. 4. Current systems associated with local auroral breakups. Planet. Space Sci. **29**, 431–447, 1981

Boyd, J.S., Belon, A.E., Romick, G.J.: Latitude and time variations in precipitated electron energy inferred from measurements of auroral height. J. Geophys. Res. **76**, 7694–7700, 1971

Brekke, A., Doupnik, J.R., Banks, P.M.: A preliminary study of the neutral wind in the auroral E region. J. Geophys. Res. **78**, 8235–8250, 1973

Cahill, L.J. Jr., Greenwald, R.A., Nielsen, E.: Auroral radar and rocket double-probe observations of the electric field across the Harang-discontinuity. Geophys. Res. Lett. **5**, 687–690, 1978

Comfort, R.H., Wu, S.T., Swenson, G.R.: An analysis of auroral E region neutral winds based on incoherent scatter radar observations at Chatanika. Planet. Space Sci. **24**, 541–560, 1976

Davis, T.N.: The morphology of the auroral displays of 1957–1958. 2. Detail analysis of Alaska data and analysis of high latitude data. J. Geophys. Res. **67**, 75–110, 1962

Ecklund, W.L., Balsley, B.B., Carter, D.A.: A preliminary comparison of F region plasma drifts and E region irregularity drifts in the auroral zone. J. Geophys. Res. **82**, 195–197, 1977

Fukushima, N.: Equivalent current pattern for ground geomagnetic effect when the ionospheric conductivity is discontinuous at the foot of a field-aligned current sheet. Rep. Ionos. Space Res. Jap. **28**, 147–151, 1974

Greenwald, R.A.: Diffuse radar aurora and the gradient drift instability. J. Geophys. Res. **79**, 4807–4810, 1974

Greenwald, R.A.: Studies of currents and electric fields in the auroral zone ionosphere using radar auroral backscatter. In: Dynamics of the magnetosphere, S.-I. Akasofu, ed.: pp. 213–248. Dordrecht: D. Reidel 1979

Greenwald, R.A., Weiss, W., Nielsen, E., Thomson, N.R.: STARE: a new radar auroral backscatter experiment in northern Scandinavia. Radio Sci. **13**, 1021–1039, 1978

Gustafsson, G.: On the orientation of auroral arcs. Planet. Space Sci. **15**, 277–294, 1967

Gustafsson, G.: Auroral orientation curves and the auroral oval. Tellus **21**, 852–860, 1969

Gustafsson, G.: A revised corrected geomagnetic coordinate system. Ark. Geofys. **5**, 595–617, 1970

Gustafsson, G., Baumjohann, W., Iversen, I.: Multi-method observations and modelling of the three-dimensional currents associated with a very strong Ps6 event. J. Geophys. **49**, 138–145, 1981

Holzworth, R.H., Berthelier, J.-J., Cullers, D.K., Fahleson, U.V., Fälthammar, C.-G., Hudson, M.K., Jalonen, L., Kelley, M.C., Kellogg, P.J., Tanskanen, P., Temerin, M., Mozer, F.S.: The large-scale ionospheric electric field: its variation with magnetic activity and relation to terrestrial kilometric radiation. J. Geophys. Res. **82**, 2735–2742, 1977

Hyppönen, M., Pellinen, R., Sucksdorff, C., Torniainen, R.: Digital all-sky camera. Techn. Rept. No. *9*, Finnish Meteorol. Inst., 1974

Inhester, B., Baumjohann, W., Greenwald, R.A., Nielsen, E.: Joint two-dimensional observations of ground magnetic and ionospheric electric fields associated with auroral zone currents. 3. Three-dimensional currents associated with a westward travelling surge. J. Geophys. **49**, 155–162, 1981

Kamide, Y., Rostoker, G.: The spatial relationship of field-aligned currents and auroral electrojets to the distribution of nightside auroras. J. Geophys. Res. **82**, 5589–5608, 1977

Kawasaki, K., Rostoker, G.. Perturbation magnetic fields and current systems associated with eastward drifting auroral structures. J. Geophys. Res. **84**, 1464–1480, 1979

Küppers, F., Untiedt, J., Baumjohann, W., Lange, K., Jones, A.G.: A two-dimensional magnetometer array for ground-based observations of auroral zone electric currents during the International Magnetospheric Study (IMS). J. Geophys. **46**, 429–450, 1979

Lassen, K., Danielsen, C.: Quiet time pattern of auroral arcs for different directions of the interplanetary magnetic field in the Y-Z-plane. J. Geophys. Res. **83**, 5277–5284, 1978

Madsen, M.M., Iversen, I.B., D'Angelo, N.: Measurements of high-latitude ionospheric electric fields by means of balloon-borne sensors. J. Geophys. Res. **81**, 3821–3824, 1976

Maurer, H., Theile, B.: Parameters of the auroral electrojet from magnetic variations along a meridian. J. Geophys. **44**, 415–426, 1978

Meng, C.-I., Holzworth, R.H., Akasofu, S.-I.: Auroral circle-delineating the poleward boundary of the quiet auroral belt. J. Geophys. Res. **82**, 164–172, 1977

Mozer, F.S., Lucht, P.: The average auroral zone electric field. J. Geophys. Res. **79**, 1001–1006, 1974

Opgenoorth, H.J., Pellinen, R.J., Maurer, H., Küppers, F., Heikkila, W.J., Kaila, K.U., Tanskanen, P.. Ground-based observations of an onset of localized field-aligned currents during auroral breakup around magnetic midnight. J. Geophys. **48**, 101–115, 1980

Rino, C.L., Brekke, A., Baron, M.J.: High resolution auroral zone E region neutral wind and current measurements by incoherent scatter radar. J. Geophys. Res. **82**, 2295–2304, 1977

Rostoker, G., Barichello, J.C.: Seasonal and diurnal variation of Ps6 magnetic disturbances. J. Geophys. Res. **85**, 161–163, 1980

Saito, T.: Some topics for the study of the mechanism of magnetospheric substorm by means of rocket observation in the auroral zone. Antarctic Rec. **43**, 65–69, 1972

Saito, T.: Examination of the models for the substorm-associated magnetic pulsation Ps6. Sci. Rep. Tohuku Univ. Ser. 5 Geophys. **22**, 35–59, 1974

Saito, T.: Long-period irregular magnetic pulsation, Pi3. Space Sci. Rev. **21**, 427–467, 1978

Theile, B., Wilhelm, K.: Field-aligned currents above an auroral arc. Planet. Space Sci. **28**, 351–355, 1980

Zanetti, L.J. Jr., Arnoldy, R.L., Cahill, L.J. Jr., Behm, D.A., Greenwald, R.A.: Comparative rocket observations of ionospheric electric fields in the auroral oval. Space Sci. Instr. **5**, 183–196, 1980

Received September 7, 1981; Revised version November 9, 1981
Accepted November 13, 1981